International Journal of Technology 14(3) 484-500 (2023)
Received July 2022 / Revised October 2022 / Accepted Ocotber 2022

International Journal of Technology

Numerical Investigation for Single-Phase and Two-Phase Flow in Duct Banks with Multi Types of Vortex Generators

Adnan Qahtan Ibrahim[1,2*], Riyadh Sabah Alturaihi[1]

[1]*Department of Mechanical Engineering, Faculty of Engineering, University of Babylon, Hilla, Babylon, 51002, Iraq*
[2]*Automotive Department, College of Engineering/AL-Musaib, University of Babylon, Hilla, Babylon, 51002, Iraq*

Abstract. This paper examines the numerical work of the thermal convection over tube banks with winglets through the heat exchanger in two parts under turbulent conditions. The first section investigates the influence of two-phase (water and air) flow on the performance of two kinds of vortex generators (Delta and Rectangular) winglets across the oval tube banks. The second section studied the performance of four types of winglets (Delta, Rectangular, Zikzak, and Sinusoidal wavy), circular and oval tubes, forward and downward configurations, and various angles of attack (15°, 20°, and 25°) in two-phase flow. Delta winglets provide the highest performance at an attack angle of 15° for oval tube banks in a two-phase flow with a moderate turbulent flow rate.

Keywords: Duct Banks; Heat exchanger; Sinusoidal winglets; Zikzak winglets

1. Introduction

In numerous industrial processes, heat convection is essential in heating and cooling operations. At high flow velocities, a two-phase flow is utilized to minimize pressure losses in the duct. Over the last two decades, researchers have focused on winglets' ability to generate interconnected vortices or swirling flow parallel to the flow orientation. These winglets have been studied to enhance the Heat convection effectiveness of various heat exchangers via air- or gas-side heat transfer. (Fiebig, 1998; Fiebig, Valencia, and Mitra, 1993) explained flow with winglets could lead to a massive increase in heat convection coefficient in the laminar duct flows, increasing transverse vortex generators (VGs). It was found that an inline tube configuration enhanced the heat convection rate by 55–65 %, with a comparable pressure drop of 20–45 %. Lau, Meiritz, and Ram (1999) published the results of an experimental work investigating the movement in a turbulent duct flow with heat and momentum using Vortex generators. Oval tubes have several advantages over circular tubes in lowering pressure drop and reducing the wake zone. As a result, when vortex generators are combined with oval tubes, it is possible to get increased thermal performance without considerably raising the pressure drop (He and Zhang, 2012). Compared to the Baseline instance, the vortex generator exhibits a promising improvement in heat convection coefficients and a significant penalty in pressure loss (Sahel, Benzeguir, and Baki, 2015). The heat convection coefficient in the region of the wake behind the tube can

*Corresponding author's email: adnan.issa@uobabylon.edu.iq, Tel.: +964-780-7386343
doi: 10.14716/ijtech.v14i3.5811

be increased by up to 240% in the addition of winglet-kind longitudinal VGs. The overall channel heat convection coefficient has significantly increased, according to the existing findings. The improvement has a lot of potential for reducing the heat exchanger size (Lu and Zhou, 2016; Tiwari *et al.,* 2003; Biswas, Mitra, and Fiebig, 1994). The overall heat transfer coefficient for both laminar and turbulent flows increases as the number of pairs of VGs increased, based on the number of rows difference (Syaiful *et al.,* 2017). The geometry of the tube banks impacts the thermo-hydraulic characteristics of a fin and tube heat exchanger (FTHE) directly (Sahel, Ameur, and Mellal, 2020) and a reduction in the heat convection coefficient as the flat tube's size increases (Sahel, Ameur, and Boudaoud, 2019). A study by Susanto *et al.* (2020) showed that the heat transfer rate improves more smoothly; where the influence of convection walls is minimal, the local Nusselt number (Nu) grows and the velocity profile increased marginally. The addition of flat vortex generators increases the heat convection coefficient by approximately 62.53% (Sahel, Ameur, and Alem, 2021). Augmentation of heat convection occurs with curved rectangular winglet VGs for flow in a rectangular channel (Naik, Tiwari, and Kim, 2022) and for flow across three rows of cylindrical tubes installed on a flat plate with height-averaged (Nu) and perimeter-averaged (Nu) variances along the height of a cylinder. (Naik and Tiwari, 2017; Naik and Tiwari, 2018). With upstream rectangular winglet pair positions, performance is improved (Naik and Tiwari, 2020a). In recent years, researchers have investigated several additional areas for vortex generator forced convection enhancement, including the addition of bulges, dimples, and punched delta winglets as vortex generators are all geometric features. The collected data indicate that a tube incidence angle of 20° is the optimal structure for eliminating the hot areas among the tubes and increasing the heat convection coefficient by 13% according to the base scenario (Abdoune *et al.,* 2021). It is known that tube diameter and height variances impact the convection heat coefficient value (Susmiati *et al.,* 2022). Inserts of various models to Vortex generators (Oneissi *et al.,* 2018; Tang et al., 2016; Boonloi and Jedsadaratanachai, 2016), the use of combined winglets (Tamna *et al.,* 2016), delta winglets with Nanofluids (Ahmed *et al.,* 2017), built-in interrupted delta-winglet (Wu *et al.,* 2016), the application of VGs to various kinds of heat exchangers (Garelli *et al.,* 2019; Song and Tagawa, 2018), and enhancement of heat convection have been documented for angles of attack ranging from 0° to 45o. In contrast, the heat convection coefficient decreases for angles of attack ranging from 135° to 180° (Afshari, Zavaragh, and Nicola, 2019). In this study, the air is used as a second phase with water to increase vortex generators' efficiency by reducing pressure loss in the duct.

2. The Geometric Model

2.1. Modelling of Flow and Boundary Condition

The characteristics of the problem and boundary condition for the single and two phase-flows can be shown in Figure 1. The rectangular duct inlet is represented as the fluid inlet's superficial velocities. The oval tube wall is exposed to constant heat flux, while the outlet pressure is represented at the outlet of the rectangular duct. The remaining portion of the duct walls is put to be adiabatic.

The heat convection coefficient and the temperature distribution were investigated in the duct by using various values for the discharges of water and air with different shapes and positions of the vortex generators. ANSYS-Fluent 19.0 is used to evaluate the flow characteristics of water flow and mixture (water-air) flow through the banks of the tubes with vortex generators. Fluent shows temperature distribution, pressure gradient, and velocity for two-phase and single-phase flow through the tube banks.

Fluent is a fluid flow simulation software suite that solves fluid flow problems using computational fluid dynamics (CFD). It solves a fluid's governing equations by using the finite volume method. Fluent's fluid problem scheme is defined by momentum, mass, and energy conservation laws. This law defines a finite volume-based discretization of a partial differential equation. These parameters pass in the course of the rectangular duct for fluid flow over oval tube banks with and without winglets. Computational fluid dynamics (CFD) is the branch of fluid dynamics that investigates the issue by calculating and giving practical methods for reproducing natural flow by solving the governing equations numerically (Abdulnaser, 2009).

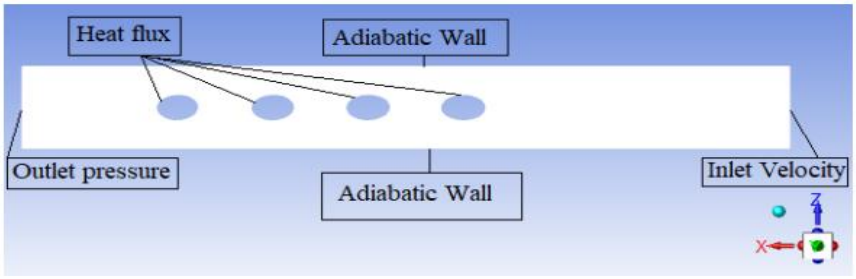

Figure 1 Boundary Condition

The boundary conditions of the single-phase and two-phase flow systems are presented in Table 1.

Table 1 Boundary conditions

Zone	Fluid	Energy
Inlet	Velocity	293 k
Tube walls	No-slip	21883.8 w/m^2
Duct walls	Symmetry	Symmetry
Winglets	No-slip	Adiabatic
Outlet	Pressure	Adiabatic

2.2. The Geometry of the Testing Section

In order to simulate the system, it has been modeled as a 3-D model using Solid Works 2018 combined with Ansys Workbench 19.0. The model has been drawn as a rectangular shape, and its dimensions are (12 cm × 2 cm × 100 cm). The geometry of the testing section is set to be fluid, as shown in Figure 2. Using the diameter of the tube (D) as the characteristic length scale, all dimensions of the duct are calculated as L = 10D, W = 1.2D, and H = 0.2 D, respectively.

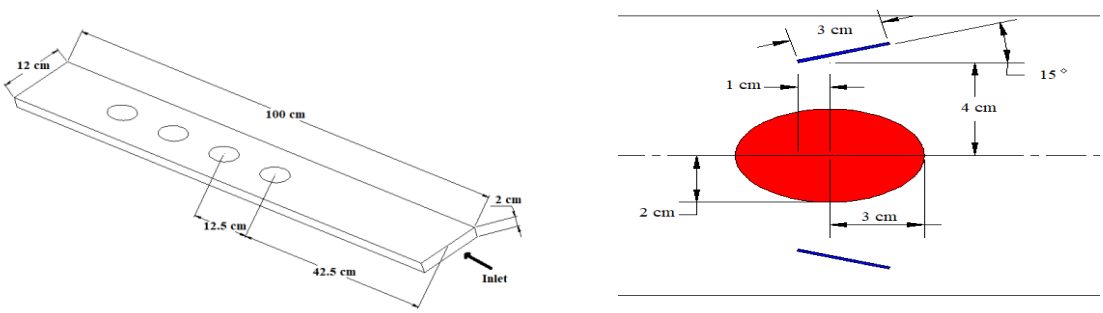

(a) (b)

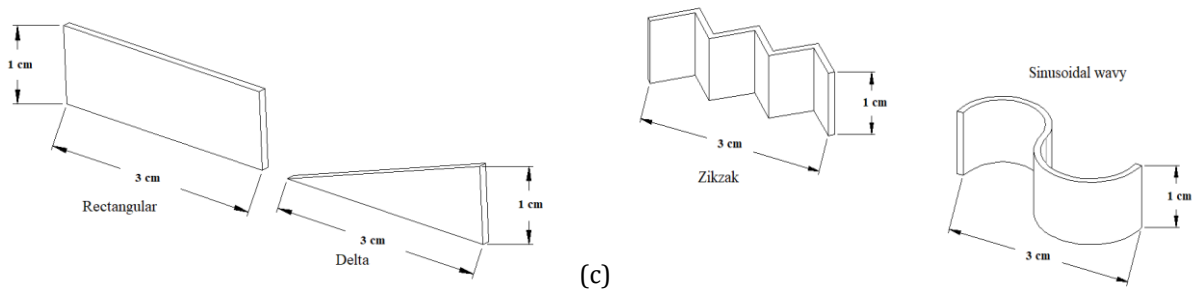

(c)

Figure 2 (a) Computational domain for test section; (b) Vortex generator placement with oval tube; (c) Four types of vortex generators

2.3. Mesh Generation

Because there are so many mesh types to choose from, it is essential to consider factors like flow field, geometry, and complexity when choosing which mesh to use. The required CPU time, solution accuracy, and convergence rate are all influenced by the size and kind of mesh (Bakker, 2006). In this work, the meshing procedure is performed in the Ansys Workbench 19.0 application using Quadrilateral structured grid elements. The meshing sizes for maximum and minimum meshing sizes are set to be equal (0.001 m) for oval and circular tubes, as shown in Figure 3. Table 2 shows how many elements and nodes each situation in this study contains for oval and circular tubes, respectively.

Table 2 The number of elements and nodes

Case	Nodes No.	Elements No.
Without Vortex	202860	181440
Delta	124767	624620
Rectangular	124831	624663
Zikzak	124826	624657
Sinusoidal	134436	674249

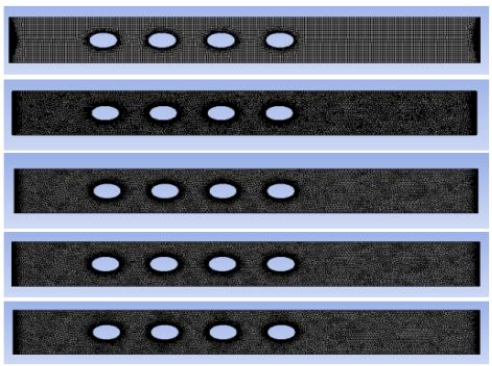

Figure 3 The Mesh of oval tubes

2.4. Grid independence

A grid-independent solution is required to enhance the precision of the computations. The present work on grid independence consists of three parts: convergence index, grid refinement, and General Richardson. Two various winglet positions relative to the center of each tube are used. For forward ($\Delta X = -1, \Delta Y = \pm 4$), downward ($\Delta X = 1, \Delta Y = \pm 4$) of each tube with $\alpha = 15°$ and $Re = 3643.5$.

3. Governing Equations

The challenge entails solving the flow field and heat convection problems associated with a bank of oval and circular tubes fitted with winglets in a rectangle duct under a transient state. Vortex generators are added to the duct to improve heat transfer. A computational examination is necessary because of how their addiction impacts the flow field and heat convection. The flow field must be resolved to establish the ideal heater diameter and form for the vortex generators.

3.1. Continuity Equation

$$\frac{\partial}{\partial t}(\rho_m) + \nabla.(\rho_m \vec{v}_m) = 0 \tag{1}$$

3.2. Momentum Equation

$$\frac{\partial}{\partial t}(\rho_m \vec{v}_m) + \nabla.(\rho_m \vec{v}_m \vec{v}_m) = -\nabla p + \nabla.[\mu_m(\nabla \vec{v}_m + \nabla \vec{v}_m^T)] + \rho_m \vec{g} + \vec{F} + \nabla.[\sum_{k=1}^{n} \alpha_k \rho_k \vec{v}_{dr,k} \vec{v}_{dr,k}] \tag{2}$$

3.3. Energy Equation

$$\frac{\partial}{\partial t}\sum_{k=1}^{n}(\alpha_k \rho_k E_K) + \nabla.\sum_{k=1}^{n}(\alpha_k \vec{v}_k (\rho_k E_k + p)) = \nabla.(k_{\text{eff}} \nabla T) + S_E \tag{3}$$

4. Turbulence Model

Models are utilized to have the capacity for characterizing and predicting the physics of the multiphase flow. Also, these models are suitable for different applications that have multiphase flow. Some demonstrating approaches are the Euler-Lagrange approach, the Volume of fluid approach, the Euler-Euler approach, and dispersed phase modeling. The Euler-Lagrange method is computationally expensive and is appropriate for flows with a small volume percentage of the dispersed phase. The (k-ω) standard model is utilized in place of the (k-ε) model in this work due to the (k-ε) model's poor prediction of rotating and swirling flows, as well as fully developed flows in the rectangular ducts (Shbeeb and Mahdi, 2016).

Also, the (k-ω) standard turbulence model will be used to simulate the flow-through test section. The single and two-phase flows are modeled by combining the model with various parameters based on the testing factors and the outcomes of the experiments to compare and validate the CFD results (Vejahati *et al.*, 2009; Fluent, 2006).

$$\frac{\partial(\rho u_j k)}{\partial x_j} = P_k - \beta^* \rho \omega k + \frac{\partial}{\partial x_j}\left[\left(\mu + \frac{\mu_t}{\rho_k}\right)\frac{\partial k}{\partial x_j}\right] \tag{4}$$

$$\frac{\partial(\rho u_j \omega)}{\partial x_j} = \alpha \frac{\omega}{k} P_k - \beta \rho \omega^2 + \frac{\partial}{\partial x_j}\left[\left(\mu + \frac{\mu_t}{\rho_\omega}\right)\frac{\partial \omega}{\partial x_j}\right] \tag{5}$$

5. Performance parameter

$$j = St.Pr^{2/3} \tag{6}$$

$$f = \frac{\Delta p}{\frac{\rho v^2}{2}\frac{A_t}{A_{min}}} \tag{7}$$

where j is the Colburn factor, and f is the coefficient of friction (Chu, He, and Tao, 2009).

6. Model validation

The computational fluid dynamics model validation by numerical simulations of flow through the heat exchanger with an intake of the Reynolds number between 600 and 3000 were compared to the numerical outcomes of (Fiebig, Valencia, and Mitra, 1993).

The maximum errors between the present model findings and the numerical outcomes of (Fiebig, Valencia, and Mitra, 1993) are 4.35% for *Nu* and 5.825% for *f*. The model validation results are shown in Figure 4. From the above analyses, the high degree of agreement between these outcomes illustrates the model's reliability in precisely forecasting the flow structure and heat convection properties.

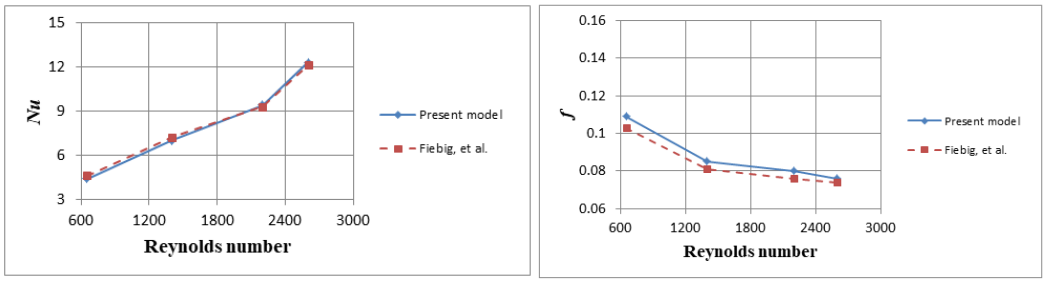

(a) (b)

Figure 4 Validation of the present model with the germane work (Fiebig, Valencia, and Mitra, 1993) for various values of Re (a) *Nu* and (b) *f*

7. Results and Discussion

Figures 5 to 19 show the numerical results of the increased water-air flow rates on the temperature gradient at various locations in the duct with a constant electrical power of (110 W) as a heat flux. In this study, the performance of VGs was investigated based on the temperature gradient between the fluid flow and the surface of the tube bank, which corresponded to the pressure loss inside the duct. The best performance at the lowest temperature difference and the lowest pressure drops, with other parameters remaining kept constant. The Nusselt number (*Nu*) was directly proportional to the coefficient of heat convection. When the temperature gradient between single or two-phase flow and the surfaces of tube banks increased, the heat convection coefficient decreased, and vice versa. Also, the friction coefficients (*f*) were directly proportional to the pressure drop in the duct, according to Equation 7.

7.1. Effect of the phase

7.1.1. Single-phase flow

Figure 5 illustrates the temperature gradient between water flow and oval tube surfaces at various locations in the duct without winglets, with Delta winglets, and with Rectangular winglets for three different water flow rates (15, 17.5, and 20 L/min). Observed from this figure that the temperature gradient decreased as the water flow rate increased. These results agree with Chu, He, and Tao (2009), and Haque and Rahman (2020) for reduced temperature gradient at the water flow velocity increased; therefore, the heat convection coefficient increased. When the water flow rate increases, the flow velocity increases, ultimately enhancing the heat convection coefficient.

Figure 6 illustrates the entrance and exit pressure for water flow at many points in the duct without winglets, with Delta winglets, and with Rectangular winglets for three different water flow rates (15, 17.5, and 20 L/min). The pressure loss in the duct raised as the discharge of water increased, and these results agree with Chu, He, and Tao (2009).

When the water flow rate increases, the pressure drop decreases, which reduces the coefficients of friction.

Adding vortex generators to the duct can augment the heat convection coefficient by raising the velocity of single-phase flow and the turbulence intensity within the duct. As the flow velocity increases, the temperature gradient reduces. When flow is oriented toward the oval tube's surface, the temperature gradient is inversely proportional to flow velocity.

Figure 7a illustrates the fluctuation of a temperature gradient with Reynolds number in water flow across the bank of oval tubes without winglets generators. Owing to a decrease in the temperature gradient between the water flow and surfaces of the oval tube, the heat convection coefficient improved as the Re number raised.

Figure (7b) represents the fluctuation of the pressure reduction with Reynolds number in water flow over oval tube banks without winglets. As the Reynolds number grew, the duct pressure losses were reduced.

Figure (7c) represents the Reynolds number performance parameter for water flow over oval tube banks without winglets. As the Re number climbed, the performance parameter improved because the pressure in the duct and the temperature gradient between the water flow and the surfaces of the oval tube decreased. The delta winglets' performance is greater than that of the other two vortex generators. These results concur with the reports of Haque and Rahman (2020), and Naik and Tiwari (2020b) which examined the influence of different vortex generator forms on heat flow in the duct and showed that Delta winglets provide the highest performance.

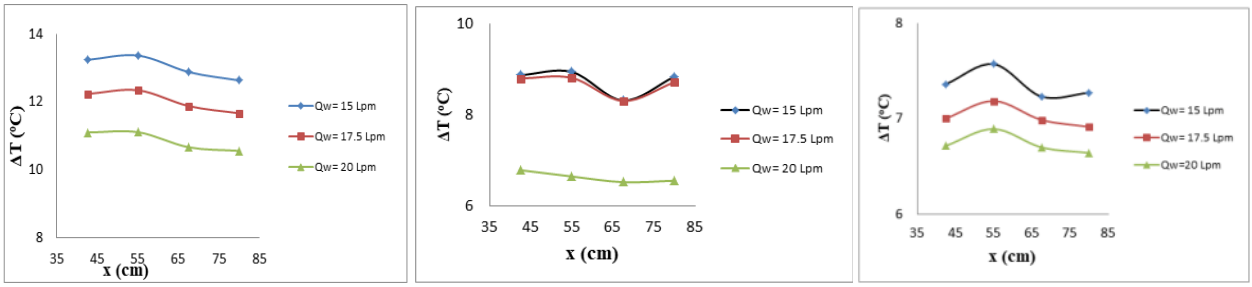

(a) (b) (c)

Figure 5 The temperature gradient between water flow and surfaces of an oval tube for various water flow rates (15, 17.5, and 20 L/min) for single-phase flow (a) without winglets (b) with Delta winglets (c) with Rectangular winglets

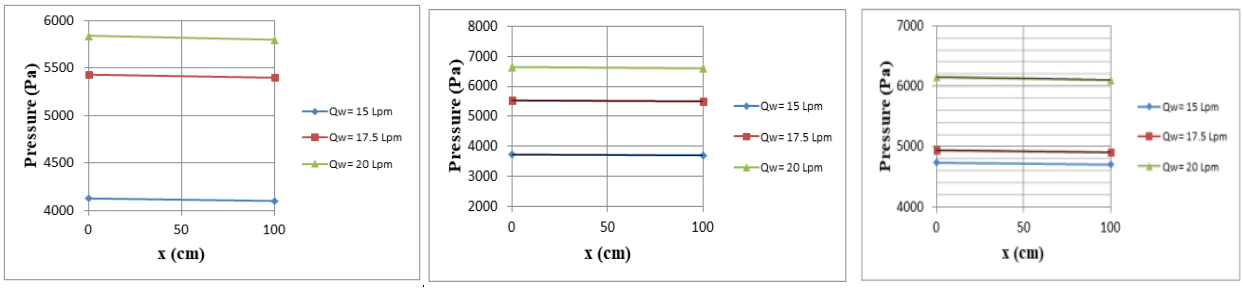

(a) (b) (c)

Figure 6 Inlet and Outlet pressure in the duct with an oval tube for single-phase flow (a) without winglets (b) with Delta winglets (c) with Rectangular winglets

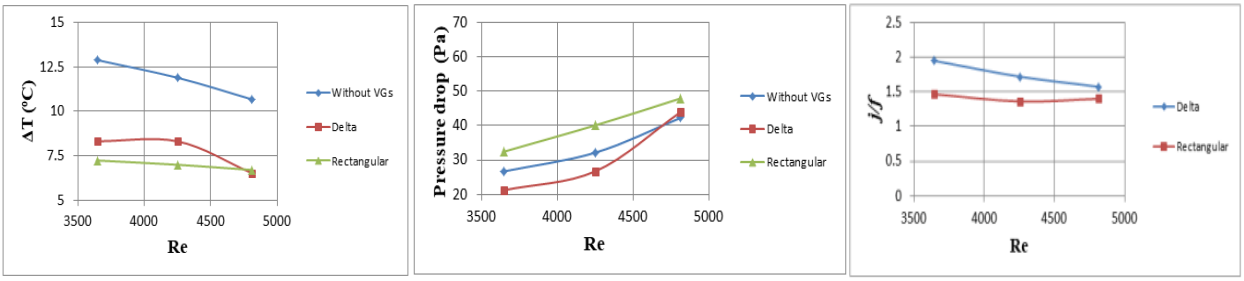

(a) (b) (c)

Figure 7 (a) The temperature gradient with Delta and Rectangular winglets for single-phase flow over oval tube (b) Pressure drop (c) Performance parameter

7.1.2. Two-phase flow

Figure 8 indicates that at a constant discharge of water, the temperature gradient between mixture (water-air) flow and surfaces of oval tubes increased. At these points, the airflow rate increases (8.33, 16.67, and 25 L/min) with a constant water flow and heat flux. When the flow rate of water and air flow is increased without winglets, the heat convection rate drops, and the temperature gradient becomes less significant. The heat convection coefficient improved as the temperature difference reduced because the winglets concentrated the working fluid on the tube surface with Delta winglets and Rectangular winglets used in the duct.

Figure 9 represents the inlet and outlet pressure in the duct for water-air flow at various points. At these points, the airflow rate increases (8.33, 16.67, and 25 L/min) with a constant flow rate of water and heat flux. The pressure losses without winglets in the duct are reduced. Increased pressure drops compared to Delta winglets, and Rectangular winglets are used in the duct that is not utilized. In addition, the pressure drops in the duct are minimized due to growth in the flow rate of water-air Delta winglets. This is in accordance with the findings of Chu, He, and Tao (2009) and Haque and Rahman (2020).

In addition, the pressure drop is reduced when the discharge of mixture (water-air) flow is increased in the absence of winglets. When rectangular VGs are used in the duct, the pressure losses are more significant than not. In addition, when the flow rate of water-air increases with rectangular winglets, the pressure losses in the duct are decreased. There is good agreement with that of Haque and Rahman (2020) and Naik and Tiwari (2020b).

Adding winglets to the duct can raise the surface velocity of water-air flow, raising the heat convection coefficient by generating intense turbulence. The temperature gradient decreases as the flow velocity increases. When the flow is directed toward the surfaces of the oval tube, the temperature gradient is inversely related to the flow velocity. The airflow rate increased from (8.33, 16.67, and 25 L/min) with a constant flow rate of water and heat power of (110 W).

The effect of the Reynolds number for water-air flow over oval tube banks in a turbulent region on heat convection rate and pressure reduction is essential for optimal design and location of vortex formation. Due to the decrease in pressure and temperature gradient between water-air flow and surfaces of the oval tube in the duct, the performance parameter was improved when the Re number of water was lowered. The Re number of air grew as the air flow rate raised (8.33, 16.67, and 25 L/min), but the water flow rate remained constant.

The variance of the temperature gradient with Re number in water-air flow over oval tube banks without winglets, with Delta winglets, and with Rectangular winglets are represented in Figure 10. At a constant flow rate of water, the heat convection coefficient

increases as the temperature gradient between the water-air flow and surfaces of the oval tube decreases.

The variance of the drop in pressure with the Re number in water-air flow over oval tube banks without winglets, with Delta winglets, and with Rectangular winglets are visualized in Figure 11. When the Re number of water and air increased, the pressure drop decreased in the duct with a constant flow rate of water.

The variance between the Re number and performance parameter in the water-air flow over oval tube banks with and without winglets is depicted in Figure 12. As water-air flow increased, the performance parameter improved. Delta winglets offer the most efficient performance. This is in agreement with the findings by Chu, He, and Tao (2009).

Figures 13,14, and 15 illustrate that the velocity contour for water flow and water-air flow without winglets, with Delta winglets, and with Rectangular winglets are used in the duct from Workbench 19.0 (ANSYS - Fluent 19.0) when a flow rate of air increases (0, 8.33, 16.67, and 25) (L/min) respectively, with a constant flow rate of water.

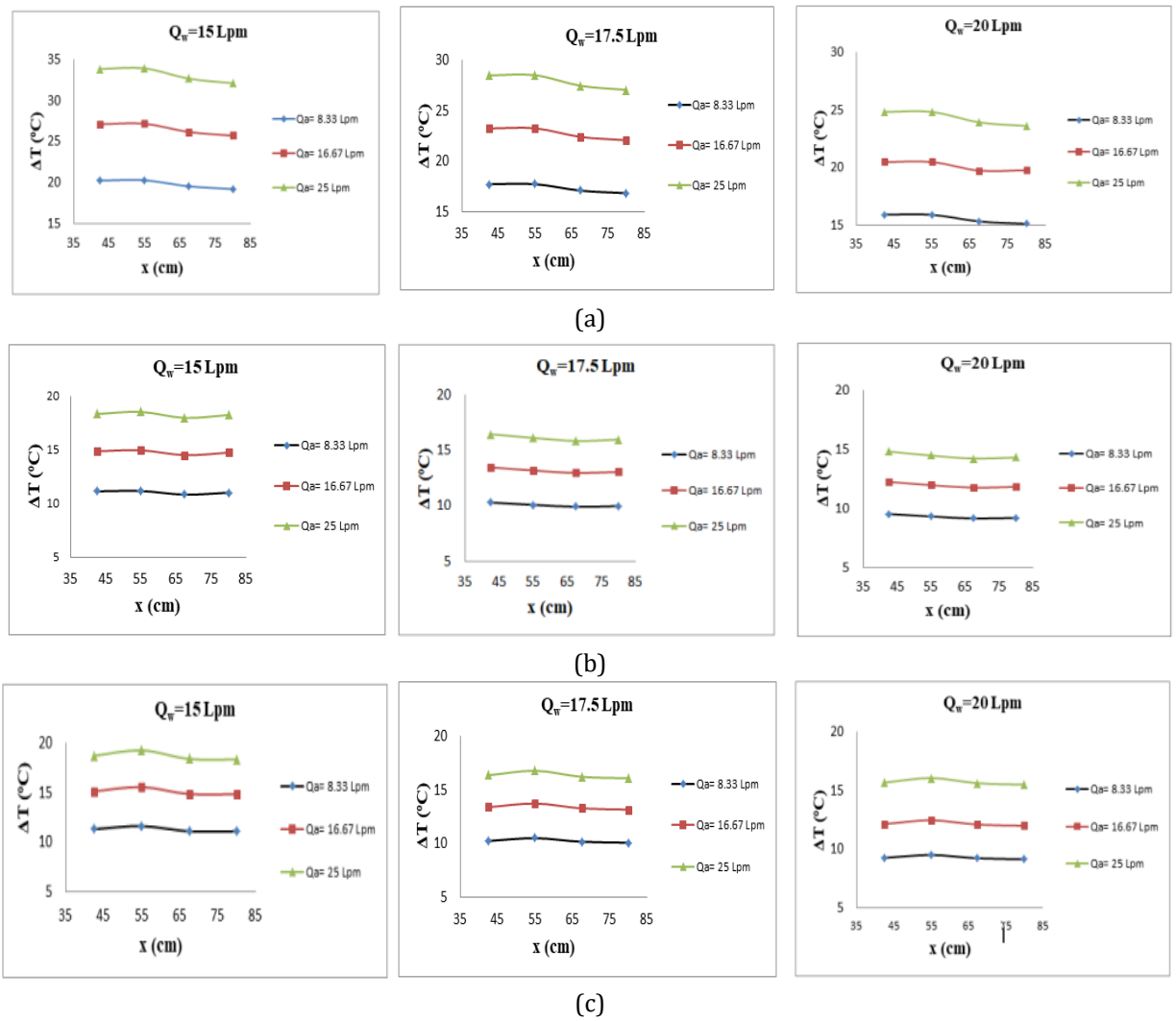

Figure 8 The temperature gradient between the flow of water and air with oval tube surfaces for two-phase flow (a) without winglets (b) with Delta winglets (c) with Rectangular winglets

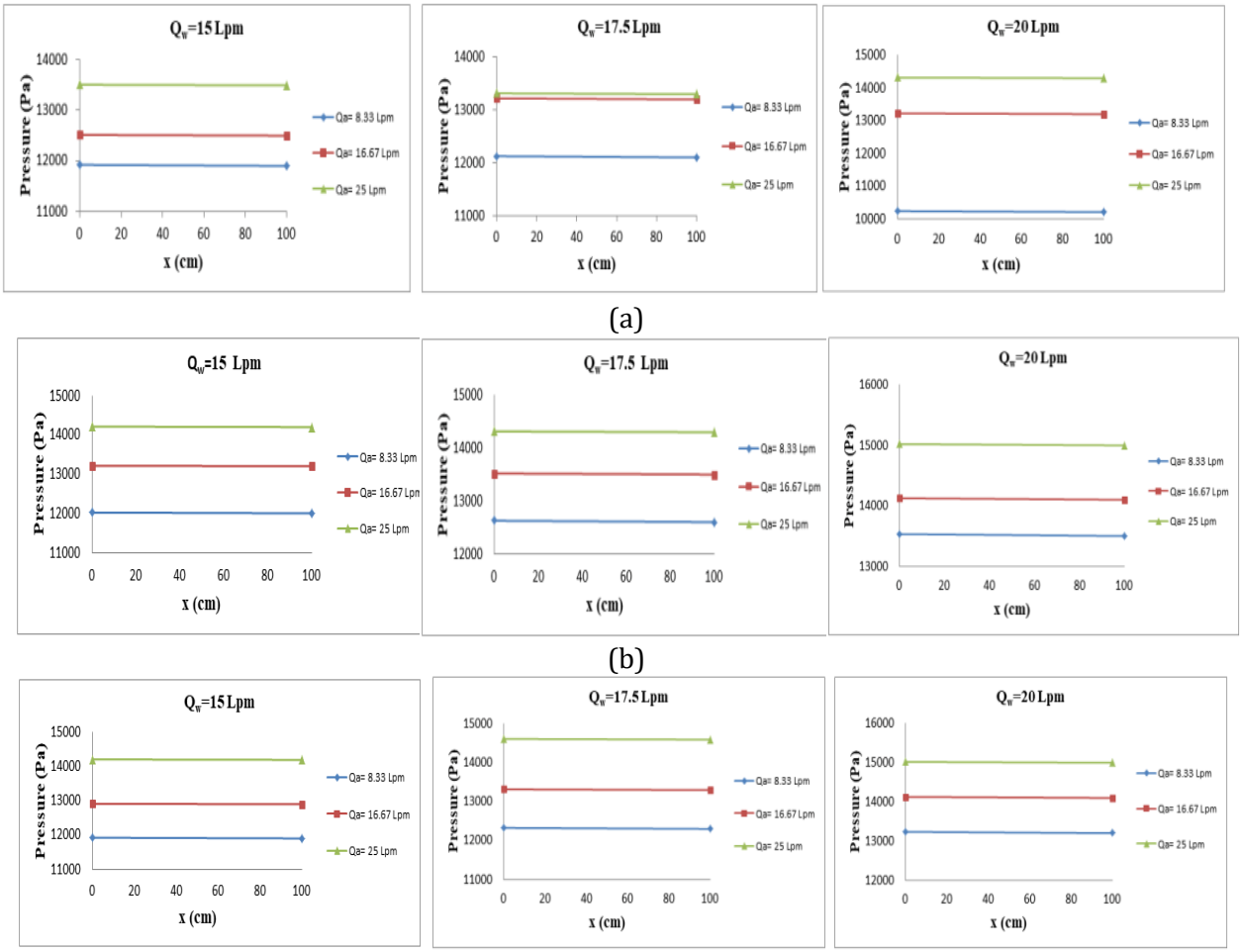

Figure 9 Inlet and Outlet pressure in the duct with an oval tube for two-phase flow (a) without winglets (b) with Delta winglets (c) with Rectangular winglets

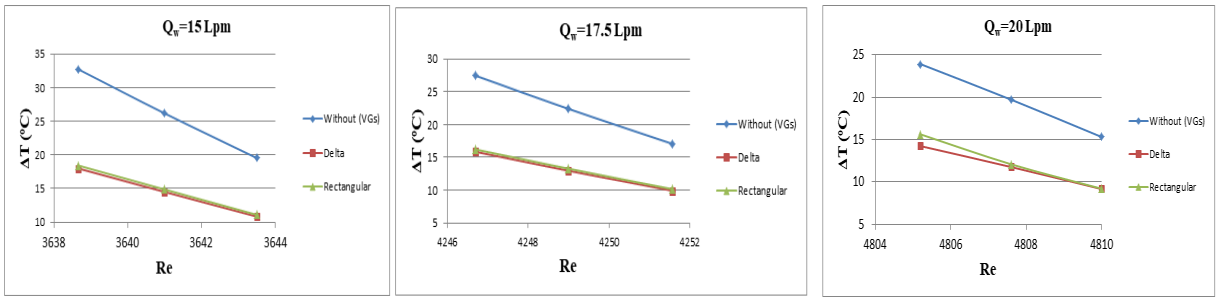

Figure 10 The temperature gradient with Delta and Rectangular winglets for two-phase flow over oval tube at (a) Q_w= 15 L/min (b) Q_w= 17.5 L/min (c) Q_w= 20 L/min

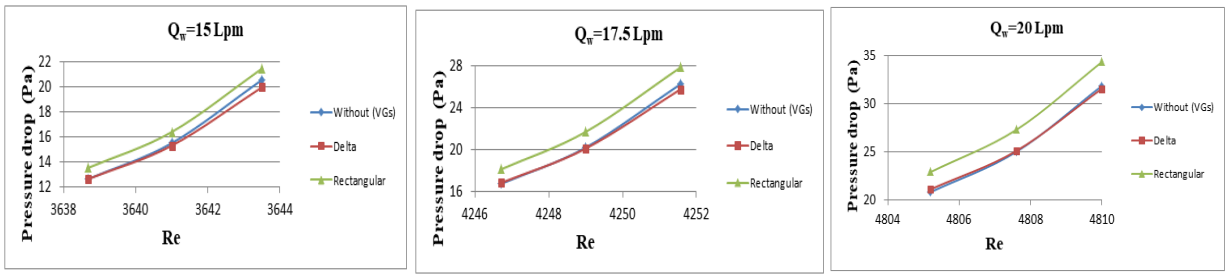

(a) (b) (c)

Figure 11 Pressure drop with Delta and Rectangular winglets for two-phase flow over oval tube at (a) Q_w= 15 L/min (b) Q_w= 17.5 L/min (c) Q_w= 20 L/min

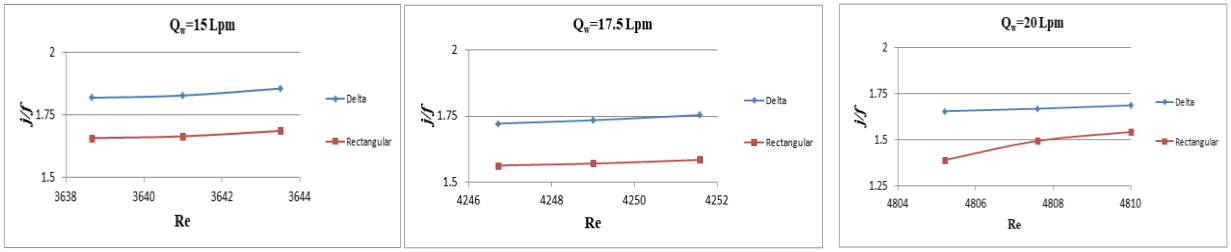

(a) (b) (c)

Figure 12 Performance parameter with Delta and Rectangular winglets for two-phase flow over oval tube (a) Q_w= 15 L/min (b) Q_w= 17.5 L/min (c) Q_w= 20 L/min

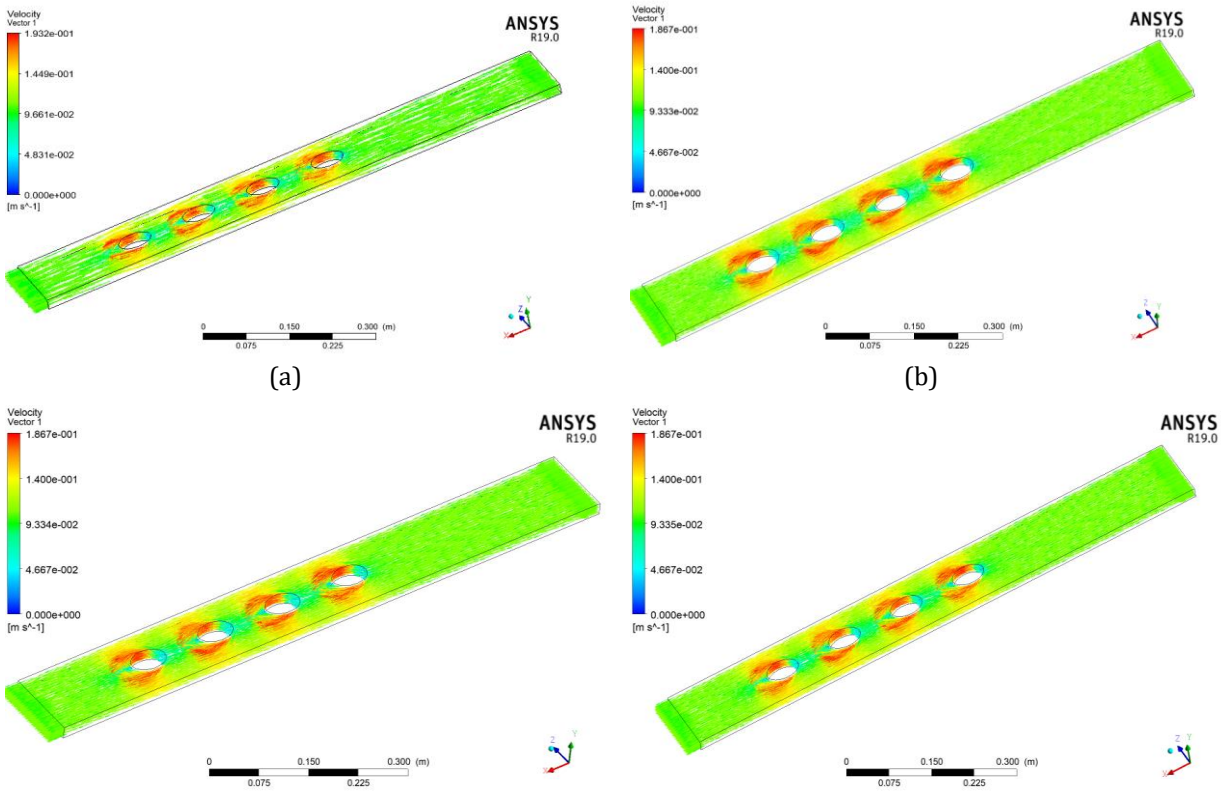

(a) (b)

(c) (d)

Figure 13 The velocity vector without vortex generators (a) single-phase flow (b) two-phase flow at constant a flow rate of water 15 Lpm with a flow rate of air 8.33 Lpm (c) 16.67 Lpm (d) 25 Lpm

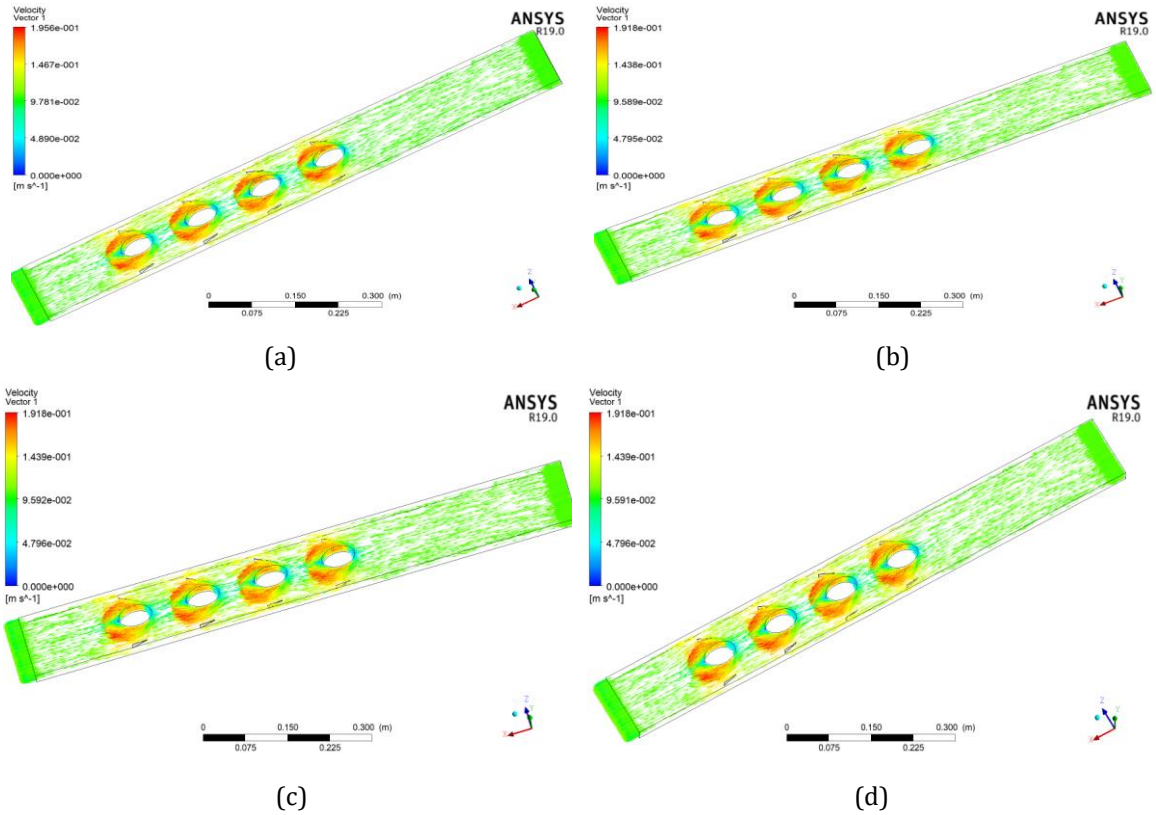

Figure 14 The velocity vector with delta winglets as vortex generators (a) single-phase flow (b) two-phase flow at constant a flow rate of water 15 Lpm with a flow rate of air 8.33 Lpm (c) 16.67 Lpm (d) 25 Lpm

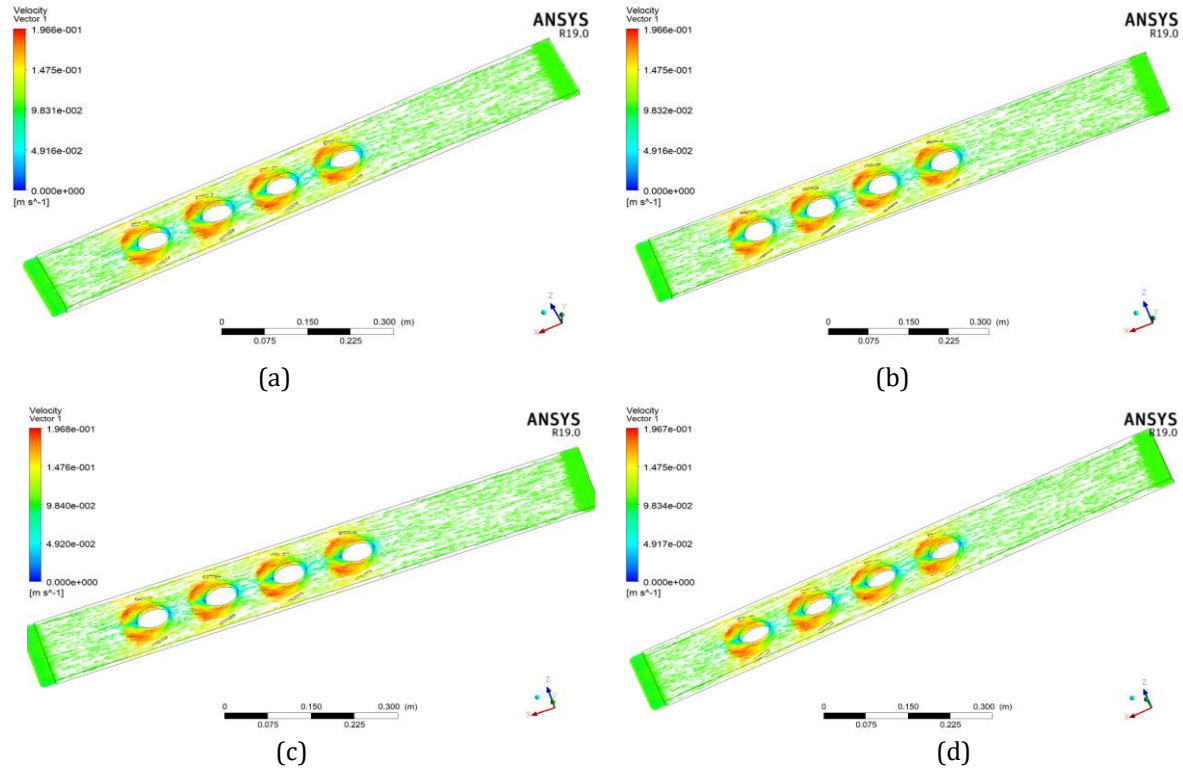

Figure 15 The velocity vector with rectangular winglets as vortex generators (a) single-phase flow, (b) two-phase flow at constant a flow rate of water 15 Lpm with a flow rate of air 8.33 Lpm (c) 16.67 Lpm (d) 25 Lpm

7.2. Effect of the position, an angle of attack, and the configuration of vortex generators

Four shapes of vortex generators (Delta, Rectangular, Zikzak, and Sinusoidal wavy) winglets are investigated numerically. Workbench 19.0 is used to compute the results and analyzes for turbulent two-phase flow area. Other parameters are used in this investigation of the oval and circular tube banks, forward and downward configurations, and the (k-ω) standard model is used.

Figures 16 and 17 show the temperature gradient between water-air flow and surfaces of the circular and oval tube at various points in the duct. Figures 18 and 19 illustrate the inlet and outlet pressure in the duct at many angles of attack for circular and oval tube banks, respectively.

Figures 20 and 21 show the performance parameter at various positions in the duct at many angles of attack for circular and oval tube banks, respectively. The performance of Delta winglets in the forward configuration is higher than the other winglets, and these results agree with Haque and Rahman (2020), Naik and Tiwari (2020c), and Chu, He, and Tao (2009.

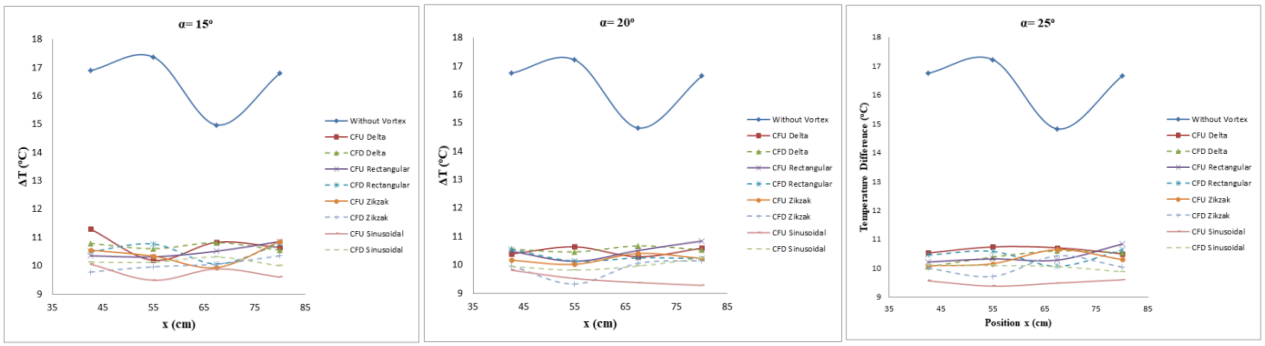

(a) (b) (c)

Figure 16 The temperature gradient for circular tube banks in two-phase flow at an angle of attack (a) 15°, (b) 20°, (c) 25°

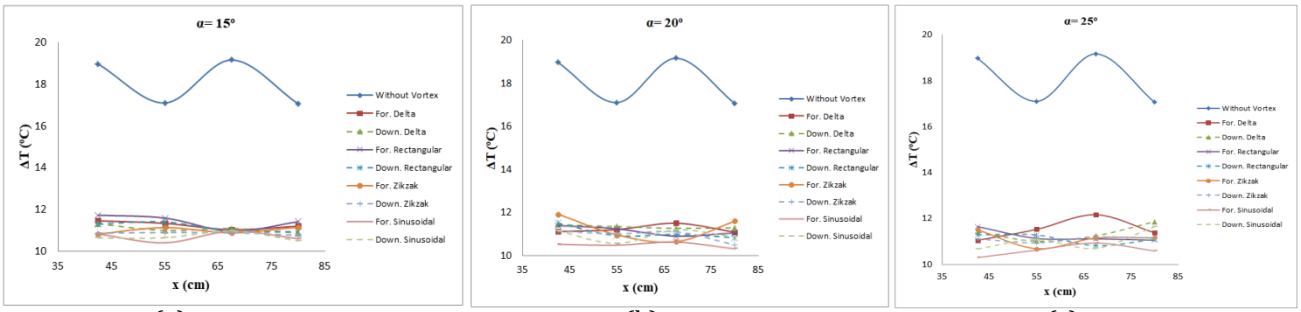

(a) (b) (c)

Figure 17 The temperature gradient for oval tube banks in two-phase flow at an angle of attack (a) 15°, (b) 20°, (c) 25°

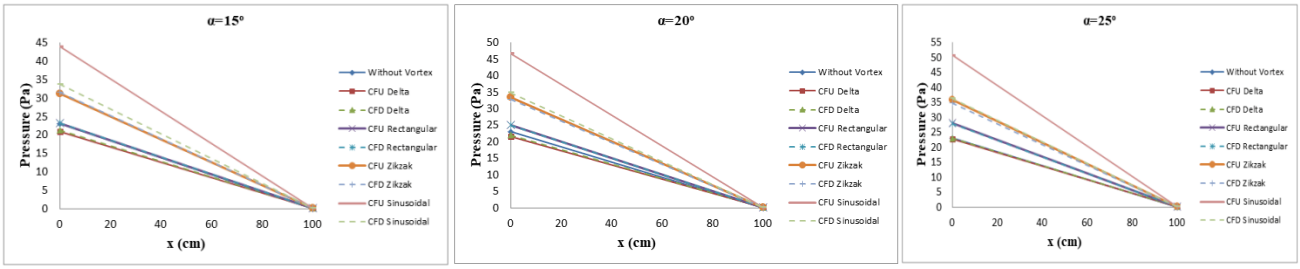

(a) (b) (c)

Figure 18 Inlet and Outlet pressure in the duct for circular tube banks in two-phase flow at an angle of attack (a) 15°, (b) 20°, (c) 25°

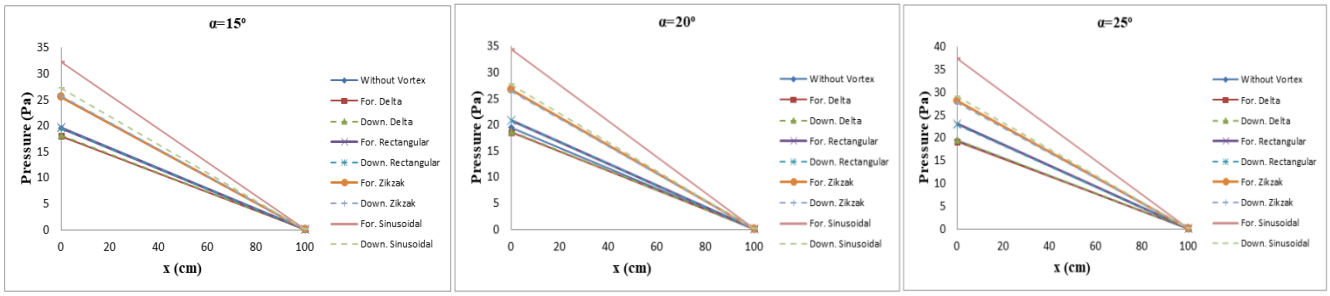

(a) (b) (c)

Figure 19 Inlet and Outlet pressure in the duct for oval tube banks in two-phase flow at an angle of attack (a) 15°, (b) 20°, (c) 25°

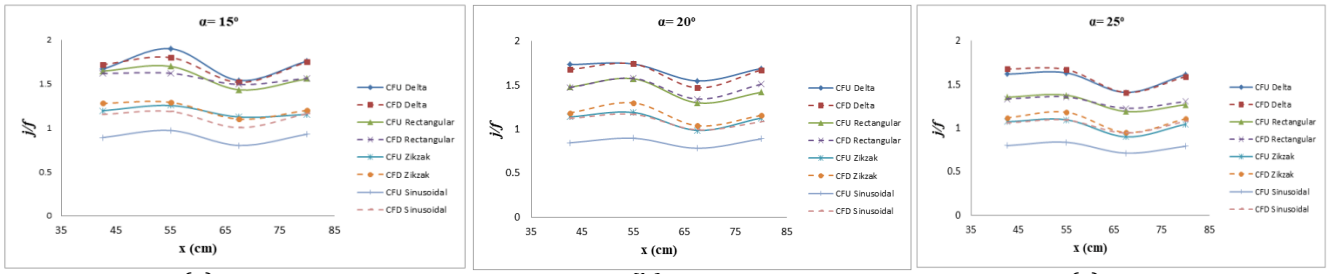

(a) (b) (c)

Figure 20 Performance parameter for circular tube banks in two-phase flow at an angle of attack (a) 15°, (b) 20°, (c) 25°

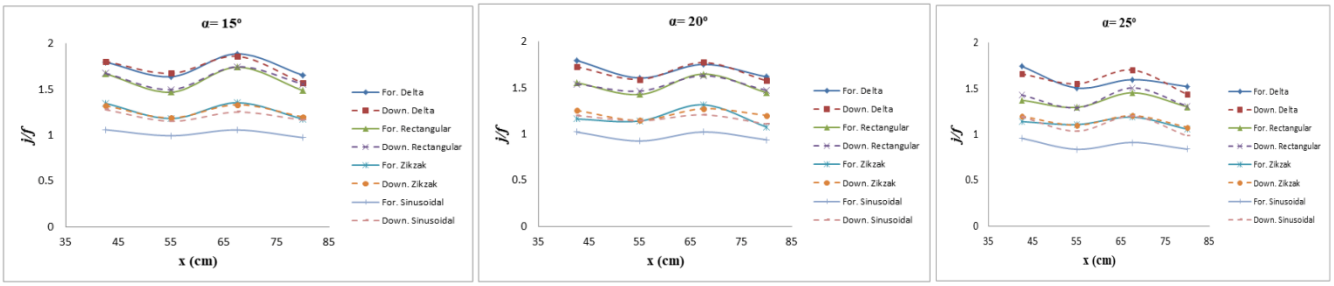

(a) (b) (c)

Figure 21 Performance parameter for oval tube banks in two-phase flow at an angle of attack (a) 15°, (b) 20°, (c) 25°

8. Conclusions

When water-air flow rates are increased in the absence of winglets, the heat convection rate reduces due to the temperature gradient for the mixture flow and the tubes' bank surface raises with less intensity, reducing the pressure loss in the duct. In water-air flows with delta and rectangular winglets, the heat convection coefficient increases as the water and air flow rates increase. As the temperature difference decreases, the pressure loss in the duct also decreases.

Comparing the absence and presence of winglets in the water flow across oval tube banks, as the Re number raised, the performance parameter decreased due to a large fall in pressure within the duct as the temperature gradient for the water flow and wall of tube decreased. The performance of delta winglets is greater than that of other vortex generators. In water-air flows across tube banks with and without vortex generators, the discharge of air increases while the water discharge remained unchanged. The performance parameter decreases substantially as the pressure within the duct is reduced and the temperature gradient for the water-air flow and tube bank surfaces increases. The performance of delta VGs is higher than that of other kinds of (VGs). Delta winglets perform

optimum at a 15° angle of attack for banks of oval tubes in two-phase flow with a moderately turbulent flow rate due to the lowest pressure loss in the duct relative to the other two angles of attack, which corresponds to an increase in heat convection. Researchers should continue to develop novel designs for vortex generators in future work in this field by investigating their shape, length, height, and position.

Acknowledgments

I want to express my gratitude to my supervisor, Dr. Riyadh S. Al-Turaihi, for his assistance throughout my time at the University of Babylon. Additionally, I would like to express my gratitude to the faculty and staff of the University of Babylon, Faculty of Engineering, Mechanical Engineering department for their assistance and education.

References

Abdoune, Y., Djamel, S., Redouane, B., Karima, A., 2021. Convective Heat Transfer and Fluid Flow Characteristics in Fin and Oval-Tube Heat Exchanger. *Journal of Mechanical Engineering and Sciences,* Volume 15(2), pp. 7936–7947

Abdulnaser, S., 2009. *Computational Fluid Dynamics*. Hanbook, Academic Press

Afshari, F., Zavaragh, H.G., Nicola, G.D., 2019. Numerical Analysis of Ball-Type Turbulators in Tube Heat Exchangers with Computational Fluid Dynamic Simulations. *International Journal of Environmental Science and Technology*, Volume 16(7), pp. 3771–3780

Ahmed, H.E., Yusoff, M.Z., Hawlader, M.N.A., Ahmed, M.I., Salman, B.H., Kerbeet, A.S., 2017. Turbulent Heat Transfer and Nanofluid Flow in a Triangular Duct with Vortex Generators. *International Journal of Heat and Mass Transfer*, Volume 105, pp. 495–504

Bakker, A., 2006. Applied Computational Fluid Dynamics, Mesh Generation. Computational Fluid Dynamics Lectures. Available online at https://docslib.org/doc/4700816/lectures-on-applied-computational-fluid-dynamics, Accessed on April 22, 2021

Biswas, G., Mitra, N.K., Fiebig, M., 1994. Heat Transfer Enhancement in Fin-Tube Heat Exchangers by Winglet Type Vortex Generators. *International Journal of Heat and Mass Transfe*, Volume 37(2), pp. 283–291

Boonloi, A., Jedsadaratanachai, W., 2016. Flow Topology, Heat Transfer Characteristic and Thermal Performance in a Circular Tube Heat Exchanger Inserted with Punched Delta Winglet Vortex Generators. *Journal of Mechanical Science and Technology*, Volume 30(1), pp. 457–471

Chu, P., He, Y., Tao, W., 2009. Three-Dimensional Numerical Study of Flow and Heat Transfer Enhancement Using Vortex Generators in Fin-and-Tube Heat Exchangers. *Journal of Heat Transfer*, Volume 131(9), p. 091903

Fiebig M.A, 1998. Vortices Generators and Heat Transfer. *Chemical Engineering Research and Design,* Volume 76(2), pp. 108–123

Fiebig, M.A, Valencia, Mitra, N.K., 1993. Wing-Type Vortex Generators for Fin-and-Tube Heat Exchangers. *Experimental Thermal and Fluid Science*, Volume 7(4), pp. 287–295

ANSYS FLUENT 12.0 User's Guide, 2009. Modeling Multiphase Flows. Available online at https://wwwafs.portici.enea.it/project/neptunius/docs/fluent/html/ug/node718.htm, Accessed on March 5, 2021

Garelli, L., Rodriguez, G.L., Dorella, J.J., Storti, M.A., 2019. Heat Transfer Enhancement in Panel Type Radiators Using Delta-Wing Vortex Generators. *International Journal of Thermal Sciences*., Volume 137, pp. 64–74

He, Y.L., Zhang, Y., 2012. Chapter Two-Advances and Outlooks of Heat Transfer Enhancement by Longitudinal Vortex Generators. *Advances in Heat Transfer*, Volume 44, pp. 119–185

Lau, S., Meiritz, K., Ram, V.I.V., 1999. Measurement of Momentum and Heat Transport in the Turbulent Channel Flow with Embedded Longitudinal Vortices. *International Journal of Heat and Fluid Flow*, Volume 20(2). pp. 128–141

Lu, G., Zhou, G., 2016. Numerical Simulation on Performances of Plane and Curved Winglet-Pair Vortex Generators in a Rectangular Channel and Field Synergy Analysis. *International Journal of Thermal Sciences*, Volume 109, pp. 323–333

Haque, M.R., Rahman, M.A., 2020. Numerical Investigation of Convective Heat Transfer Characteristics of Circular and Oval Tube Banks with Vortex Generators. *Journal of Mechanical Science and Technology*, Volume 34(1), pp. 457-467

Naik, H., Tiwari, S., 2017. Heat Transfer Enhancement Due To Curved Winglet Pairs in Fin-Tube Heat Exchangers. Proceedings of the 24th National and 2nd International ISHMT-ASTFE Heat and Mass Transfer Conference (IHMTC-2017), pp. 385–392

Naik, H., Tiwari, S., 2018. Effect of Aspect Ratio and Arrangement of Surface-Mounted Circular Cylinders on Heat Transfer Characteristics. Journal of Enhanced Heat Transfer, Volume 25(4-5), pp. 443–463

Naik, H., Tiwari, S., 2020a. Numerical Investigations on Fluid Flow and Heat Transfer Characteristics of Different Locations of Winglets Mounted in Fin-Tube Heat Exchangers. *Thermal Science and Engineering Progress*, Volume 22, p. 100795

Naik, H., Tiwari, S., 2020b. Thermal Performance Analysis of Fin-Tube Heat Exchanger with Staggered Tube Arrangement in Presence of Rectangular Winglet Pair's. *International Journal of Thermal Sciences*, Volume 161, p. 106723

Naik, H., Tiwari, S., 2020c. Thermodynamic Performance Analysis of an Inline Fin-Tube Heat Exchanger in Presence of Rectangular Winglet Pairs. *International Journal of Mechanical Sciences*, Volume 193, p. 106148

Naik, H., Tiwari, S., Kim, H.D., 2022. Flow and Thermal Characteristics Produced by a Curved Rectangular winglet Vortex Generator in a Channel. International Communications in Heat and Mass Transfer, Volume 135

Oneissi, M., Habchi, C., Russeila, S., Lemenandb, T., Bougeard, D., 2018. Heat Transfer Enhancement of Inclined Projected Winglet Wair Vortex Generators with Protrusions. *International Journal of Thermal Sciences*, Volume 134, pp. 541–551

Sahel, D., Ameur, H., Alem K., 2021. Enhancement of the Hydrothermal Characteristics of Fin-and-Tube Heat Exchangers by Vortex Generators. Journal of Thermophysics and Heat Transfer, Volume 35(1), pp. 152–163

Sahel, D., Ameur, H., Boudaoud, W., 2019. A New Correlation for Predicting the Hydrothermal Characteristics over Flat Tube Banks. Journal of Mechanical and Energy Engineering, Volume 3(43), pp. 273–280

Sahel, D., Ameur, H., Mellal, M., 2020. Effect of Tube Shape on the Performance of a Fin and Tube Heat Exchanger. Journal of Mechanical Engineering and Sciences, Volume 14(2), pp. 6709–6718

Sahel, D., Benzeguir, R., Baki, T., 2015. Heat Transfer Enhancement in a Fin and Tube Heat Exchanger with Isosceles Vortex Generators. Mechnika, Volume 21(6), pp. 457–464

Shbeeb, A.A., Mahdi, A., 2016. Assessment of Various Turbulance Models in Displacement Ventilation System for Prediction of Airflow and Temperature Distribution with Experimental Data. *Journal of Kerbala University*, Volume 12(1), pp. 8–26

Song, K.W., Tagawa, T., 2018. The Optimal Arrangement of Vortex Generators for Best Heat Transfer Enhancement in Flattube-Fin Heat Exchanger. *International Journal of Thermal Sciences*, Volume 132, pp. 355–367

Susanto, E., Alhamid, M.I., Nasruddin, Budihardjo, Prabowo, Novianto, S., 2020. Characteristics of Air Flow and Heat Transfer in Serpentine Condenser Pipes with Attached Convection Plates in Open Channel. *International Journal of Technology*. Volume 11(3), pp. 564–573

Susmiati, Y., Purwantana, B., Bintoro, N., Rahayoe, S., 2022. Heat Transfer Characteristics in Vertical Tubular Baffle Internal Reboiler through Dimensional Analysis. *International Journal of Technology*. Volume 13(3), pp. 508–517

Syaiful, A., Soetanto, M.F., Siswantara, A.I., Bae, M., 2017. Thermo-Hydrodynamics Performance Analysis of Fluid Flow through Concave Delta Winglet Vortex Generators by Numerical Simulation. *International Journal of Technology*, Volume 8(7), pp. 1276–1285

Tamna, S., Kaewkohkiat, Y., Skullong, S., Promvonge, P., 2016. Heat Transfer Enhancement in Tubular Heat Exchanger with Double V-Ribbed Twisted-Tapes. *Case Studies in Thermal Engineering*, Volume 7, pp. 14–24

Tang, L.H., Chu, W.X., Ahmed, N., Zeng, M., 2016. A New Configuration of Winglet Longitudinal Vortex Generator to Enhance Heat Transfer in a Rectangular Channel. Appl. Therm. Eng., Volume 104, pp. 74–84

Tiwari, S., Maurya, D., Biswas, G., Eswaran, V., 2003. Heat Transfer Enhancement in Cross-Flow Heat Exchangers using Oval Tubes and Multiple Delta Winglets. *International Journal of Heat and Mass Transfer*, Volume 46, pp. 2841–2856

Vejahati, F., Mahinpey, N., Ellis N., Nikoo M. B., 2009. CFD Simulation of Gas–Solid Bubbling Fluidized Bed: A New Method for Adjusting Drag Law. *Canadian Society for Chemical Engineering*, Volume 87, pp. 19–30

Wu, X.H., Yuan, P., Luo, Z.M., Wang L.X., Lu, Y.L., 2016. Heat Transfer and Thermal Resistance Characteristics of Fin with Builtin Interrupted Delta Winglet Type. *Heat Transfer Engineering*, Volume 37(2), pp. 172–182